


Folic acid-modified reverse micelle-lipid nanocapsules overcome intestinal barriers and improve the oral delivery of peptides

Jibiao He^a, Ruihuan Ding^a, Yuping Tao^a, Zhenyu Zhao^b, Ranran Yuan^b, Houqian Zhang^b, Aiping Wang^a, Kaoxiang Sun^a, Youxin Li^{a,c} and Yanan Shi^b 

^aSchool of Pharmacy, Key Laboratory of Molecular Pharmacology and Drug Evaluation (Yantai University), Ministry of Education, Collaborative Innovation Center of Advanced Drug Delivery System and Biotech Drugs in Universities of Shandong, Yantai University,, Yantai, P. R. China; ^bSchool of Life Science, Yantai University, Yantai, P. R. China; ^cState Key Laboratory of Long-acting and Targeting Drug Delivery System, Luye Pharmaceutical Co., Ltd., Yantai, P. R. China

ABSTRACT

The oral absorption of exenatide, a type 2 diabetes medication, can be increased by employing lipid nanocapsules (LNC). To increase mucus permeability and exenatide intestinal absorption, reverse micelle lipid nanocapsules (RM-LNC) were prepared and their surface was modified with DSPE-PEG-FA. The RM-LNC with surface modification of DSPE-PEG-FA (FA-RM-LNC) were able to target enterocytes and reduce mucus aggregation in the intestine. Furthermore, *in vitro* absorption at different intestinal sites and flip-flop intestinal loop experiments revealed that LNCs with surface modification significantly increased their absorption efficiency in the small intestine. FA-RM-LNC delivers more drugs into Caco-2 cells *via* caveolin-, macrophagocytosis-, and lipid raft-mediated endocytosis. Additionally, the enhanced transport capacity of FA-RM-LNC was observed in a study of monolayer transport in Caco-2 cells. The oral administration of exenatide FA-RM-LNC resulted in a prolonged duration of hypoglycemia in diabetic mice and a relative bioavailability (BR) of up to 7.5% in rats. In conclusion, FA-RM-LNC can target enterocytes and has promising potential as a nanocarrier for the oral delivery of peptides.

ARTICLE HISTORY

Received 9 January 2023
Revised 13 February 2023
Accepted 13 February 2023

KEYWORDS

Folic acid; targeted drug delivery; lipid nanocapsules; oral administration; reverse micelle

1. Introduction

Biologically active proteins and peptides play a prominent role in clinical settings owing to their high degree of selectivity and potency in addition to their relative safety and well-tolerability (Fosgerau & Hoffmann, 2015). The study of peptides for drug research and development has garnered increasing attention, with more peptide-based therapeutic products being developed (Lau & Dunn, 2018). Notably, peptides (e.g. exenatide) have shown significant performance in the treatment of diabetes. GLP-1 analogs enhance hyperglycemia-induced insulin secretion, inhibit glucagon secretion during hyperglycemia, decelerate gastric emptying to prevent large increases in postprandial blood glucose, reduce calorie intake and body weight and have no inherent risk of hypoglycemic episodes (Nauck et al., 2021). The administration of GLP-1 analogs *via* injection is a recommended mode for glucose lowering. Although peptides and proteins have excellent therapeutic potential, they present significant challenges in terms of drug delivery (Jain et al., 2019; Jain, 2020). Currently, a majority of protein-peptide-based drug formulations on the market are administered frequently by intravenous or subcutaneous injection, which greatly reduces patient compliance (Zaman et al., 2019). Therefore, this

studies focus on identifying non-injectable delivery routes, with oral delivery being the major focus (Drucker, 2020). However, oral delivery also presents challenges associated with the structural organization and physiological function of the gastrointestinal tract.

These drugs must overcome various barriers including enzymes, mucus and epithelium before they can reach circulation (Haddadzadegan et al., 2022). Therefore, the oral delivery of peptides and proteins *via* oral nanocarriers can be considered a suitable option. Lipid nanocapsules (LNC) are a promising nano-delivery vehicle prepared by the phase inversion temperature (PIT) method, which is a simple and low-energy preparation process that does not use organic solvents (Nasr & Abdel-Hamid, 2015). The nanoparticles can be controlled in terms of uniform size and are highly stable. The particles can be modified in various forms to obtain desirable delivery properties (Huynh et al., 2009). LNC can be administered in varying routes to treat a wide variety of diseases, with oral delivery being considered the most effective. LNCs improve drug transport in the mucus layer and stabilize the particle properties over a long period (Groot et al., 2013). Furthermore, the LNC surface material also protects the particles from mucin interference in the mucus

layer. Moreover, LNCs are majorly endocytosed by Caco-2 cells and can be transported intact to the extracellular compartment, thereby increasing drug uptake by the epithelial tissue (Roger et al., 2009, 2017). Notably, LNCs can deliver both hydrophilic and lipophilic drugs. Thus, it is feasible to prepare a reverse micelle to encapsulate a hydrophilic drug and then incorporate it into LNCs for delivery (Radwan et al., 2020).

Despite the significant effects of oral administration effects, it remains vital to develop new strategies to improve the ability of LNCs in delivering GLP-1 analogues to facilitate their clinical translation. Many studies report that LNCs with surface PEGylation alter the biodistribution of the particles and exhibit longer circulation times and good structural stability after intravenous injection (Laine et al., 2014). Additionally, LNCs can be modified on the surface to improve drug delivery efficiency by post-insertion methods. 1, 2-Distearoyl-sn-glycero-3-phosphoethanolamine-Poly(ethylene glycol) (DSPE-PEG) is a commonly used modification material that can be inserted into the shell of LNCs (Topin-Ruiz et al., 2021). Furthermore, therapeutic molecules or antibodies can be coupled to DSPE-PEG to achieve synergistic or targeting effects *via* post-insertion methods (Labrak et al., 2022). Among the different receptors expressed in the gastrointestinal tract, folate (FA) receptors are abundant and can improve the absorption and transport of bioactive substances in the gastrointestinal tract (Agrawal et al., 2014). Additionally, folic acid supplementation may be required for patients with diabetics having long-term metformin use (Valdes-Ramos et al., 2015). Moreover, a significant upregulation in the expression of FA transporters in the intestine of diabetic rats, which could mediate the absorption of FA-modified nanoparticles and thus exhibit significant bioavailability, has been reported (Li et al., 2022).

In this study, we aim to prepare exenatide reverse micelle lipid nanocapsules (RM-ELNC) by adding exenatide reverse micelles to the oily core of LNC (Tsakiris et al., 2019). Furthermore, to enable the targeted delivery of the particles and extend their circulation time *in vivo*, folic acid-modified exenatide reverse micelle lipid nanocapsules (FA-RM-ELNC) could be prepared by modifying DSPE-PEG-FA on the surface of the particles by post-insertion. This study also aims to compare the efficiency of the two nanocapsules as oral exenatide carriers before and after modification.

2. Materials and methods

2.1. Materials

Labrafac[®]WL1349, Phospholipon90H and Kolliphor[®]HS15 were obtained from Shanghai Macklin Biochemical Technology Ltd (Shanghai, China). 1,2-distearoyl-sn-glycero-3-phosphoethanolamine-N-(folate(polyethylene glycol)2000) (DSPE-PEG2000-FA) was obtained from Chongqing Yusi Pharmaceutical Technology Ltd (Chongqing, China). The exenatide kit was obtained from Hangzhou Qiyu Biotechnology Ltd (Zhejiang, China). Fetal bovine serum and Dulbecco's Modified Eagle Medium were obtained from Wuhan Punosai Life Sciences Ltd (Hubei, China). Db/db type II diabetic mice and Sprague–Dawley (SD) rats were obtained from Jiangsu

Jizui Pharmaceutical Biotechnology Co Ltd (Jiangsu, China). 1,1'-Diocetadecyl-3,3,3',3'-Tetramethylindodicarbocyanine,4-Chlorobenzenesulfonate Salt (DID) was obtained from Biyuntian Biotechnology Ltd (Shanghai, China).

2.2. Preparation and characterization of LNCs

2.2.1. Preparation of reverse micelles LNCs (RM-LNC)

RM-ELNCs comprised reverse micelles encapsulating exenatide (RM-EXE) and LNCs (Tsakiris et al., 2019). The RM-EXE were prepared by mixing Span[®]80 and Labrafac[®]WL1349 in a 1:5 wt/wt ratio and then dropping 30 μ L of the drug solution under high-speed stirring. Following this, LNCs were prepared using the PIT method. A mixture of 268.75 mg Labrafac[®]WL1349, 26.8 mg Phospholipon[®]90H, 206.1 mg SlutoI[®]HS15, 30 mg NaCl and 0.7344 mL ultrapure water was stirred for 3 min. Then, three gradual heating/cooling cycles (50–75 $^{\circ}$ C) were performed. In the final cycle, when the temperature was approximately 8–10 $^{\circ}$ C above the phase inversion zone, 300 μ L of preheated reverse micelles were added to the mixture. Finally, 3.625 mL of cool water (0–4 $^{\circ}$ C) was added, stirred for 5 min, then filtered through a 0.22 μ m filter membrane and refrigerated. Blank reverse micelle LNCs were prepared using the same process with the addition of a drug-free solution for preparation.

2.2.2. Preparation of DID-labeled RM-LNCs

DID-labeled RM-LNC (DID-RM-LNC) was prepared by adding DID to RM-LNC (Xu et al., 2020a). A total of 0.1 mL (10 mg/mL) of DID and 268.75 mg Labrafac[®] WL1349 was added to the vial, which was heated in a water bath until the organic solvent had completely evaporated. The mixture was then cooled to room temperature and the above preparation process was continued with the addition of the other ingredients used for the preparation of RM-LNC.

2.2.3. Preparation of DSPE-PEG-FA-modified RM-LNCs

DSPE-PEG2000-FA modified RM-LNCs were prepared using the post-insertion method (Perrier et al., 2010). A total of 750 μ L of DSPE-PEG2000-FA solution (10 mg/mL) was added to 1 mL of RM-LNC in a centrifuge tube and stirred gently for 4 h at 37 $^{\circ}$ C. The mixture was vortexed every 15 min during preparation and then cooled in an ice bath for 1 min.

2.2.4. Quantification of exenatide

Exenatide concentrations were measured using high performance liquid chromatography (HPLC; Agilent Technologies, Santa Clara, CA) using a CHIRALPAK AY-3 column (4.6 mm \times 250 mm; 3 μ m). Phase A comprised 0.5% phosphoric acid/water-acetonitrile (80:20, v/v) and phase B comprised 0.5% phosphoric acid-acetonitrile. The flow rate was maintained at 1 mL/min, while the detection wavelength was set at 210 nm and the injection volume was 20 μ L.

2.2.5. Characterization of nanoparticles

The LNC, RM-LNC and FA-RM-LNC sizes, polydispersity index (PDI) and zeta potential were characterized using a

Brookhaven nanoparticle size potential detector. The morphology of LNCs was observed using transmission electron microscopy (TEM) in a JEM-1230 system (Jeol, Tokyo, Japan). Additionally, 10 μL of the LNCs solution was dissolved in 990 μL of ultra-pure water prior to the characterization. All measurements were performed thrice.

The encapsulation efficiency (EE, %) of the loaded particles were also measured. A total of 50 μL of the LNC solution was dissolved in 950 μL of methanol and then vortexed strongly to obtain the total amount of the drug (Xu et al., 2020a). The free and encapsulated drug was separated using ultra-filtration (10 KD, 6000 rpm, 0.5 h) (Millipore, Burlington, MA). The quantification of the free and total drug was performed using the HPLC method described above.

The EE was calculated using the following formula:

$$\text{EE (\%)} = \frac{(\text{total amount of exenatide} - \text{free exenatide})}{(\text{total amount of exenatide})} \times 100.$$

2.3. LNC stability and drug release in stimulated gastrointestinal fluids

2.3.1. Stability in a simulated biological milieu

The *in vitro* physical stability of RM-LNC and FA-RM-LNC was assessed in four media: simulated gastric fluid (SGF) with and without pepsin, simulated intestinal fluid (SIF) without trypsin and phosphate-buffered solution (PBS) (Mittal et al., 2011). The effect of the gastric and intestinal fluid and PBS on the stability of LNCs was assessed based on changes in particle size and PDI (Xu et al., 2020b). Both LNCs were tested at 37°C in the above media (100 μL nanocapsules in 10 mL of medium) under gentle shaking. Sampling was performed at predetermined time points (SGF at 0, 0.5, 1, and 2 h; SIF at 0, 0.5, 1, 2, 4, and 6 h; PBS at 0, 1, 2, 3, 5, and 7 d) and analyzed using DLS in triplicates.

2.3.2. Conformational stability

The conformational stability of exenatide in different preparations was determined using circular dichroism (Chirascan VX, Applied Photophysics, Leatherhead, UK) (Agrawal et al., 2014). A total of 1 mL of exenatide solution, RM-ELNC, and FA-RM-ELNC (1 mg/mL) each were placed in dialysis bags (100 KD, Spectrum) overnight and three dialysis solutions were taken for detection. Then, a 100 μL sample was placed in a cuvette and analyzed at 190–260 nm using a 1 nm bandwidth and 1 nm step with a Time-per-point of 0.5 s. Samples were tested and baseline corrected using ultrapure water to obtain CD spectra.

2.3.3. *In vitro* release

The drug release from LNCs with or without DSPE-PEG2000-FA and exenatide solution was examined in enzyme-free SGF and SIF for 8 h, respectively. Briefly, three different solutions were placed in dialysis bags (100 KD, Spectrum) and then these bags were placed in 25 mL tubes containing 10 mL of deionized water and placed in a constant shaking water bath

at 37°C. Samples were placed in SGF (pH 1.2) for the first 2 h and then moved to the SIF media (pH 7.4) for 6 h. At predetermined times (0, 0.5, 1, 2, 3, 4, 6, and 8), 100 μL of the sample was extracted and supplemented with the same volume of release medium. Finally, cumulative release curves were drawn after measuring drug concentrations using the HPLC method described above.

2.4. *In vitro* cell studies

2.4.1. Cytotoxicity studies

The toxicity of RM-LNC and FA-RM-LNC to Caco-2 cells was measured using the Thiazolyl Blue Tetrazolium Bromide (MTT) method. Caco-2 cells were inoculated in 96-well plates at a cell density of 3×10^3 cells/well and incubated at 37°C (5% CO_2) for 24 h. The polymer concentration (0.5–10 mg/mL) of the LNC solution was substituted for the previous medium and co-culturing was continued with the cells for 24 h. The control group was cultured in a medium without the addition of polymer and cell activity was set at 100%, with three parallel groups established for each concentration. Finally, MTT solution (20 μL) was added to each group, followed by the addition of DMSO (200 μL) to dissolve the methanogenic crystals produced by the reduction of MTT in the cells. The absorbance was measured using a CYTATION imager.

2.4.2. Cellular uptake

The cellular uptake of DID-labeled RM-LNC and FA-RM-LNC (DID-FA-RM-LNC) was characterized using an imaging system. Caco-2 cells were inoculated at 3×10^4 cells/well in 24-well plates and incubated for 48 h. DID-labeled LNCs (100 ng/mL) was added to the well-plates and incubated for 1, 2, and 4 h. Cells were washed with PBS, fixed in 4% formaldehyde for 20 min and then stained for nuclei using DAPI. Finally, the cells were washed with PBS and then imaged for observation (Liang et al., 2022).

Flow cytometry was used to quantify the uptake of RM-LNCs and FA-RM-LNCs by cells. Caco-2 cells were incubated in 6-well plates at 3×10^5 /well for 48 h. Then, the cells were trypsinised after the addition of DID-labeled RM-LNC and FA-RM-LNC (5 ng/mL) for 1, 2, and 4 h. Following this, the samples were centrifuged at 1400 rpm for 6 min, resuspended in 500 μL of PBS and assayed using flow cytometry (Guo et al., 2021).

2.4.3. Investigation of cellular uptake mechanisms

Caco-2 cells were inoculated in 6-well plates at a density of 2×10^5 cells/well and incubated for 48 h. The inhibitors chlorpromazine (30 $\mu\text{mol/L}$), 5-N-ethyl-N-isopropylamine (EIPA; 20 $\mu\text{mol/L}$), formalin (20 $\mu\text{mol/L}$), and methyl B -cyclodextrin (M- β -CD; 2.5 mM) were added to the cells and incubated for 0.5 h. No inhibitors were used in the control group. DID-labeled RM-LNC and FA-RM-LNC solutions (5 ng/mL) were added to the cells and incubated for 2 h. Finally, the fluorescence intensity of the cells was measured using flow cytometry and the measurements were performed in triplicates (Zhu et al., 2016).

2.4.4. Transmembrane transport

Caco-2 cells were seeded at 1×10^5 /well in a transwell upper chamber and cultured in a cell culture incubator for approximately 21 d until the cells reached a resistance value of 300–450 Ω /cm². Then, the medium was discarded from the upper and lower chambers before initiating the experiment. The cell monolayer was washed with pre-heated Hank's Buffered Salt Solution (HBSS) and incubated in the incubator for 0.5 h. Following this, 250 μ L of DID-RM-LNCs, DID-FA-RM-LNCs, DID-RM-LNCs + DSPE-PEG-FA, and DID-FA-RM-LNCs + DSPE-PEG-FA were added to the transwell upper chamber. The concentration of DID in all LNCs was 5 μ g/mL and the concentration of free DSPE-PEG-FA was 2 mg/mL. Preheated HBSS was added to the transwell lower chamber and placed in the incubator. At predetermined time points (0.5, 1, and 3 h), samples (200 μ L) were extracted from the lateral edge of the lower chamber and supplemented with equal amounts of preheated HBSS (Sheng et al., 2016). The cumulative transfer volume was calculated after measuring the fluorescence intensity of DID in each sample. Apparent permeability (P_{app}) was calculated using the following formula:

$$P_{app} = dQ/dt \times 1 / (A \times C_0)$$

wherein dQ is the accumulated amount of DID permeating the lower chamber (μ g), A is the area of the cell monolayer (cm²) and C_0 is the initial concentration of DID in the upper chamber. Additionally, dQ/dt is the slope of the linear relationship between the accumulated transport of DID (μ g) and time (s).

2.5. In vitro intestinal experiments

2.5.1. Mucus aggregation

The fresh mucus from the rat small intestine was present uniformly over the upper chamber fibrous membrane of the transwell. A total of 1.0 mL of PBS was added to the lower chamber of the transwell, which was then balanced at 37°C for 30 min to simulate the mucus layer. After equilibration, DID-labeled RM-LNCs and FA-RM-LNCs (500 ng/mL) were added to the upper chamber of the transwell and incubated for 3 h. The PBS solution was removed from the lower chamber and the mucus layer was washed with PBS to remove the LNCs from the mucus surface. The upper chamber fibrous membrane was imaged to observe the aggregation of particles in the mucus (Liang et al., 2022).

2.5.2. Different absorption sites in the intestine

Grouped rats were fasted for 12 h and then administered DID-labeled FA-RM-LNC or RM-LNC (200 ng/mL) *via* gavage and finally euthanized 150 min after administration. Then, 1 cm sections were obtained from different intestinal sites in each group. The mesentery and fat on the surface of the intestinal segment were rinsed with PBS, then embedded in a frozen embedding medium, sectioned and observed under a fluorescent microscope (Song et al., 2019).

2.5.3. In vitro intestine penetration

Fluorescently labeled RM-LNCs and FA-RM-LNCs were prepared as solutions with concentration gradients of 1.25, 2.5, 5, 10, 20, and 40 ng/mL. The fluorescence signal of the solution was determined using 100 μ L of the sample, and the standard curve was calculated to obtain the fluorescence signal value *versus* the fluorescence concentration of the solution.

After euthanasia, the rats were dissected from the midline of the abdomen, and the duodenum, jejunum, ileum, and colon (5 cm) were placed in Tyrode's solution. Any adhering material was carefully removed from the surface of the intestinal segment and washed off using cold Tyrode's solution. Tyrode's fluid was injected into the intestinal segment, the ends were tied and the segment was completely immersed in Tyrode's fluid containing fluorescently labeled RM-LNC and FA-RM-LNC (2.5 μ g/mL). Measurements for each group were performed in triplicates. After incubation for 2.5 h, the fluorescence intensity of the solution in the intestinal ring was measured (Guo et al., 2021).

2.6. In vivo pharmacokinetics

Male SD rats (190–250 g) were fasted for 12 h and randomly divided into four groups ($n = \text{five/group}$). The subcutaneous exenatide group (*s.c.*) was administered a dose of 10 μ g/kg and sampled after 0, 5, 15, and 30 min; and 1, 2, 4, 6, 8, 10, 12, and 24 h of administration. Exenatide solution, RM-ELNCs and FA-RM-ELNCs were administered orally at a dose of 100 μ g/kg and sampled at 0, 30 min, 1, 2, 4, 6, 8, 10, 12, and 24 h after dosing. All blood samples were obtained through the orbital vein of the rat and placed in centrifuge tubes containing sodium heparin and peptidase. Blood samples were centrifuged and the supernatant was stored in a refrigerator at -80°C for further testing (Jain et al., 2012).

The exenatide levels in the plasma were measured using the exenatide ELISA kit. The blood concentration-time curve of exenatide was drawn and the relative bioavailability (BR) of the exenatide-loaded nanoparticles was calculated. The BR was calculated using the following formula:

$$\text{BR} (\%) = \text{AUC} (\text{oral}) \times \text{dose} (\text{s.c.}) / \text{AUC} (\text{s.c.}) \times \text{Dose} (\text{oral}) \times 100\%$$

where AUC is the area under the curve, oral is oral administration and *s.c.* is a subcutaneous injection.

2.6.1. Hypoglycemic activity in vivo

2.6.1.1. Single administration. The db/db diabetic mice (6 weeks old) were randomly divided into five groups ($n = 5/\text{group}$). Subcutaneous administration group was exenatide solution (10 μ g/kg). The oral administration groups were saline, exenatide solution, RM-ELNC, and FA-RM-ELNC (100 μ g/kg). Blood samples were obtained from the tail vein of mice at 0, 1, 2, 4, 6, 8, 10, 12, and 24 h after administration and blood glucose values were measured (Agrawal et al., 2014).

2.6.1.2. Multiple administrations. The same grouping and dose as described for the single dose administration was

determined for multiple dosing, once daily for the oral dosing group and twice daily (morning and evening) for the subcutaneous dosing group. Blood glucose levels were measured at predetermined time points (0, 1, 2, 3, 4, and 5d) after blood samples were collected from the tail vein.

2.7. Statistical analysis

Data are expressed as mean \pm standard deviation (SD). The statistical significance of the results was analyzed using a two-tailed student's t-test. A value of $p < .05$ was considered statistically significant, $p < .01$ was considered highly significant and $p < .001$ was considered extremely statistically significant.

3. Results

3.1. Characterization of the LNCs

As shown in Table 1, the particle size of the LNCs was found to increase by approximately 50 and 20 nm after the addition of reverse micelles and the insertion of DSPE-PEG-FA on the particle surface, respectively. The potential on the surface of the unmodified nanoparticles was negative, while that on the modified nanocapsules tended to be close to 0. Moreover, the PDI of all formulations was less than 0.2. The formulations encapsulated with exenatide had a high encapsulation rate.

TEM analysis confirmed the spherical morphology of the particles in all LNCs (Figure 1(A)). Moreover, the addition of both reverse micelles and DSPE-PEG-FA caused an increase in particle size.

3.2. In vitro drug release and stability of LNCs

The physical stability of RM-LNCs and FA-RM-LNCs was examined by measuring the PDI and particle size of the nanoparticles in four different simulated mediums at different time points (Figure 2(A)). The data showed that the PDI and particle size of both nanoparticles did not change significantly over time in the three media: SGF (with or without pepsin) and SIF (without trypsin). The particle size of both particles changed slightly in PBS after 7 d of incubation.

The graph (Figure 2(B)) shows the circular dichroism of exenatide obtained after dialysis in the exenatide solution and different preparation samples. Furthermore, the three curves significantly overlap.

As peptides are unstable in simulated gastrointestinal fluids containing enzymes, we used enzyme-free simulated gastrointestinal fluids for *in vitro* release studies (Figure 2(C)). During the first 0.5 h in SGF, the release of the formulation

group was lower than that of the solution group. After 2 h of SGF, the solution group released approximately twice as much as the formulation group. After 6 h of SIF action, the solution group achieved 71% release, while the formulation group achieved approximately 60% release. There were no significant differences observed in the overall degree of release between the two formulations. Furthermore, the release profile was smoother in the formulation group compared to the solution group.

3.3. Cytotoxicity evaluation

To investigate the cytotoxicity of RM-LNC and FA-RM-LNC after administration, we evaluated Caco-2 cell viability using the MTT method. The viability of the cells was assessed after 24 h of incubation of each of the two preparations with Caco-2 cells. As shown in Figure 3(A), the viability of the preparations used ranged from 80 to 120% after incubation with cells at concentrations between 0.5 and 8 mg/mL, indicating that both preparations had no significant effect on the viability of Caco-2 cells.

3.4. Cellular internalization and uptake mechanism

Caco-2 cells were used to examine the uptake of DID-labeled RM-LNC and FA-RM-LNC (Figure 3(B)). DID-labeled LNCs exhibited red fluorescence in the imaging system, with the FA-RM-LNC group showing a higher fluorescence intensity than the RM-LNC group at various time points. On labeling the nuclei with DAPI, we could determine that LNCs were present in the cytoplasm but not in the nuclei.

A quantitative study of the uptake of LNCs by Caco-2 cells was performed using flow cytometry. As seen in Figure 3(C), the fluorescence intensity of the FA-RM-LNC group was significantly higher than that of RM-LNC at different time points.

The mechanism of LNC uptake by cells was examined under different inhibitor conditions. LNCs were incubated with different specific inhibitors to detect the endocytic pathway. As shown in Figure 3(D), the uptake of both LNCs was inhibited at varying levels following the action of these four inhibitors. When formalin and M- β -CD were incubated with RM-LNCs, the uptake inhibition was significant, indicating that mainly caveolin- and lipid raft-mediated endocytosis were involved in the endocytosis of RM-LNCs. Contrastingly, the uptake inhibition was significant when formalin and EIPA were incubated with FA-EM-LNCs, indicating that the caveolin- and macropinocytosis-mediated endocytosis pathways are involved in the endocytosis of more modified nanocapsules.

Table 1. Size, polydispersity index (PDI), zeta potential (mV), and encapsulation efficiency (EE, %) of different formulations.

Formulations	Mean size (nm)	PDI	Zeta potential (mV)	EE (%)
LNC	60.74 \pm 2.09	0.082 \pm 0.017	-1.31 \pm 0.49	-
RM-LNC	112.26 \pm 5.18	0.098 \pm 0.016	-1.38 \pm 0.64	-
RM-ELNC	112.22 \pm 2.57	0.103 \pm 0.024	-2.29 \pm 0.25	79.73 \pm 0.59
FA-RM-LNC	131.16 \pm 3.08	0.088 \pm 0.035	0.22 \pm 0.32	-
FA-RM-ELNC	130.34 \pm 1.98	0.068 \pm 0.033	-0.31 \pm 0.42	79.12 \pm 0.25
DID-RM-LNC	111.66 \pm 4.4	0.099 \pm 0.01	-1.51 \pm 0.48	-
DID-FA-RM-LNC	132.12 \pm 2.91	0.07 \pm 0.032	0.23 \pm 0.11	-

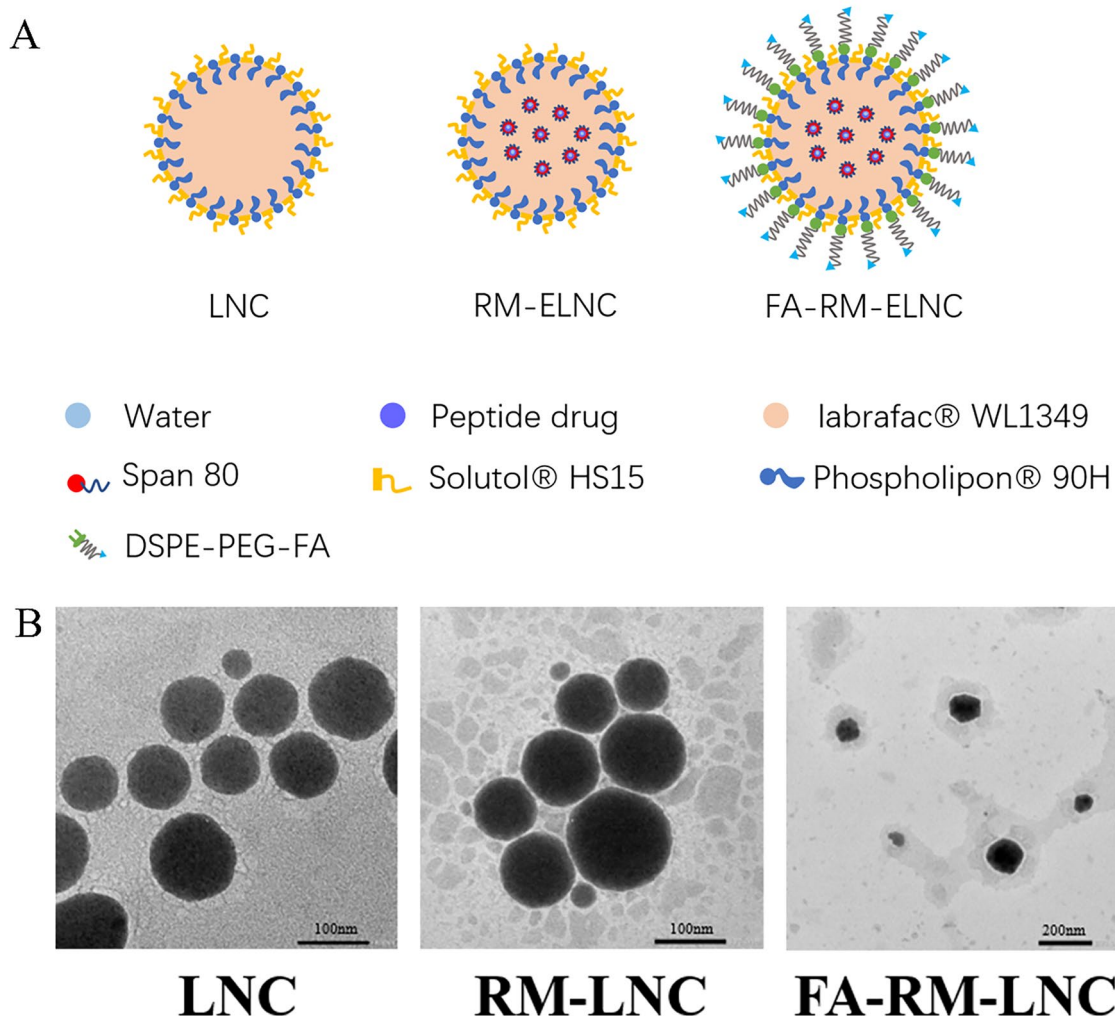


Figure 1. (A) Diagram of the LNCs, RM-ELNCs, and FA-RM-ELNCs. (B) Transmission electron micrographs of the LNCs, RM-LNCs, and FA-RM-LNCs.

3.5. *In vitro* transepithelium transport analyses

The LNCs were absorbed into the circulatory system, indicating their successful crossing of the intestinal epithelium into the bloodstream. Table 2 shows the P_{app} values for DID transport in the preparations under different conditions. The P_{app} values of the four conditions indicate that the LNCs were able to cross the cell monolayer and that the amount of permeation of surface-modified LNCs was significantly increased. To further verify the transport advantage of the DSPE-PEG-FA modification, competitive transport experiments were performed. Furthermore, the amount of DID transported was significantly lower in the DSPE-PEG-FA + FA-RM-LNC group than in the FA-RM-LNC group, with no significant difference observed in the amount of DID transported in the DSPE-PEG-FA + RM-LNC and RM-LNC groups.

3.6. Mucus aggregation and intestinal absorption

Rat intestinal mucus was uniformly spread over the transwell membrane and the aggregation of nanoparticles was observed in rat mucus using an imaging system. DID-labeled LNCs are represented in red. DID-RM-LNC showed significant

aggregation in rat intestinal mucus, while DID-FA-RM-LNC had no significant aggregation (Figure 4(A)).

We clarified the rate of absorption of LNCs in the intestine by examining the absorption in different intestinal segments of rats (Figure 4(B)). The fluorescence intensity in the duodenum was strong in both the DID-RM-LNCs and DID-FA-RM-LNCs groups, which could be attributed to the high concentration of LNCs in this region. In the jejunum, the fluorescence intensity of FA-RM-LNC was significantly stronger than that of RM-LNC, suggesting that FA-RM-LNC has a higher uptake rate than RM-LNC. The fluorescence intensity in the large intestine decreased in both groups under the effect of the harsh gastrointestinal environment and the disruption of LNCs by intestinal peristalsis, with the RM-LNC group showing a slightly higher decrease than the FA-RM-LNC group.

To further investigate the intestinal absorption of the different LNCs, a quantitative study of the intestinal absorptivity of LNCs was performed using an *in vitro* flipped intestinal loop method. The transport of FA-RM-LNCs in the duodenum, jejunum, and ileum after 2.5h was approximately 1.24, 1.37, and 1.19 times higher, respectively, than that of RM-LNCs (Figure 4(C)).

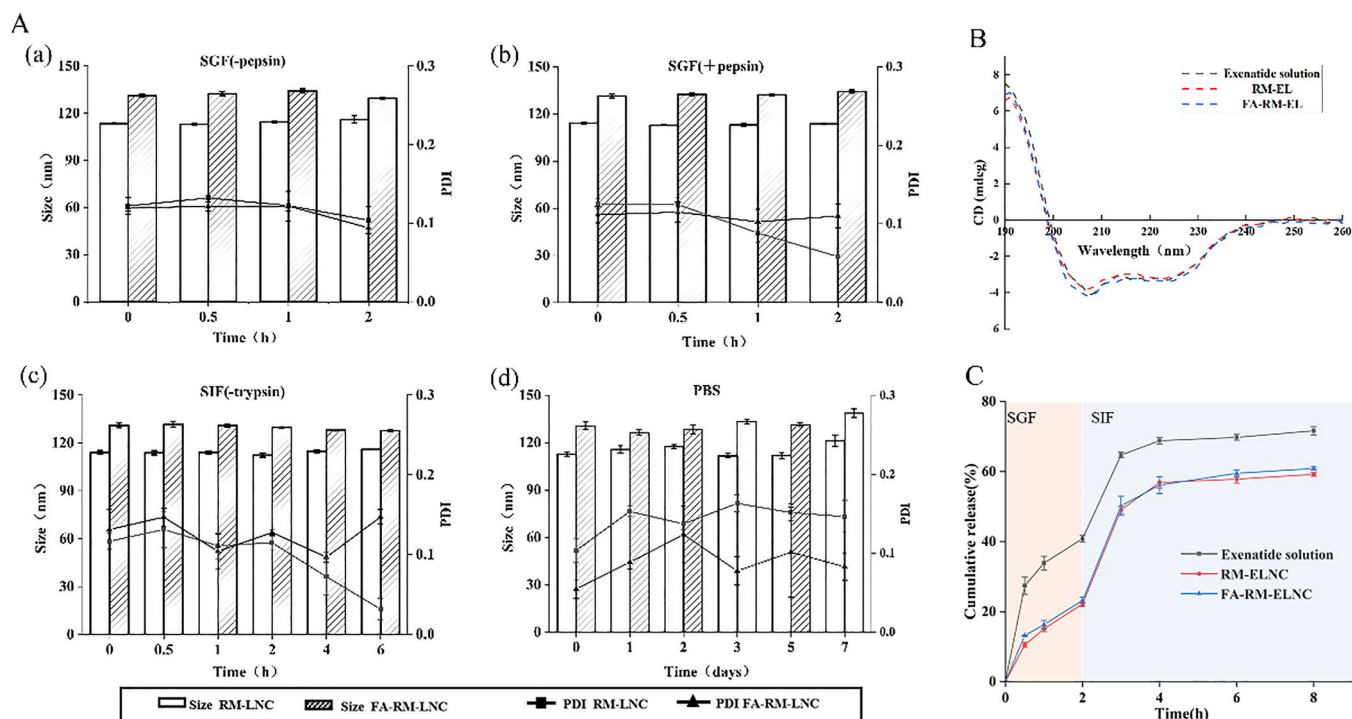


Figure 2. (A) Nanocapsule stability in biomimetic fluids. Variation in particle size and polydispersity index (PDI) of LNCs in simulated gastric fluid without pepsin, simulated gastric fluid with pepsin, simulated intestinal fluid without trypsin, and phosphate-buffered solution at predetermined time intervals (mean \pm standard deviation; $n=3$). (B) Circular dichroism spectrum of different exenatide samples. (C) Cumulative release of exenatide from exenatide solution, RM-ELNC, and FA-RM-ELNC. Data are presented as mean \pm standard deviation ($n=3$).

3.7. Pharmacokinetics

We investigated the bioavailability of orally administered RM-ELNC, FA-RM-ELNC, and exenatide solutions respectively (Figure 5(A)). The subcutaneous exenatide solution group was used as a positive control. As shown in Table 3, plasma exenatide concentrations in the oral exenatide solution group were low while that in the subcutaneous group peaked at 0.25 h. Moreover, in the oral RM-ELNC and FA-RM-ELNC groups, the peak was reached at 6 h post-dose. Additionally, the maximum blood concentration values were higher in the FA-RM-ELNC group than in the RM-ELNC group. Using subcutaneous administration as a control, the bioavailability of the oral FA-RM-ELNC group was observed to be 7.53%. Furthermore, the bioavailability of the FA-RM-ELNC group was 1.28 times higher than that of the RM-ELNC group.

3.8. Pharmacodynamics

The hypoglycemic effect after a single dose was examined. Free exenatide solution and saline did not induce hypoglycemic effects, as free exenatide is readily destroyed in the gastrointestinal tract. The subcutaneous administration of exenatide solution (10 μ g/kg) significantly reduced blood glucose values in a short period, reaching 41% of the initial value after 2 h. Notably, the treatment groups based on LNCs produced different treatment effects. As illustrated in Figure 5(B), RM-LNC reduced blood glucose to 72% after 6 h, while FA-RM-LNC had a more significant glucose-lowering effect (66%) at the same time point. Furthermore, 24 h after

FA-RM-LNC administration, the hypoglycemic level remained at 64%.

The hypoglycemic effect of the different dosing groups was tested after multiple dosings. The blood glucose levels in each group after multiple administrations are shown in Figure 5(C). No hypoglycemic effect was observed after 5 d of repeated oral exenatide solution and saline. Blood glucose levels after subcutaneous exenatide solution administration were maintained between 80 and 95%. Furthermore, blood glucose levels in the RM-ELNC group ranged from 80 to 90%. Notably, the FA-RM-ELNC group was able to maintain blood glucose levels between 65 and 90%.

4. Discussion

The addition of reverse micelles resulted in a larger oily core and a smaller proportion of surfactant in the nanoparticles, leading to a larger particle size (Aparicio-Blanco et al., 2019). Consistent with previous studies, DSPE-PEG-FA modification on the particle surface also led to an increase in particle size, which indirectly indicates the successful grafting of DSPE-PEG-FA on the particle surface. The particle sizes observed using TEM correlate well with those obtained by DLS analysis (Table 1). In the TEM image of FA-RM-LNC, the surface of the particles was not smooth, which could be due to the irregular grafting of the long chain of DSPE-PEG that causes the particles to protrude from the surface (Figure 1(B)). Nanoparticles close to about 100 nm and hydrophilic electroneutral facilitate the penetration of mucus and epithelial cell layers into the blood circulation (Guo et al., 2021).

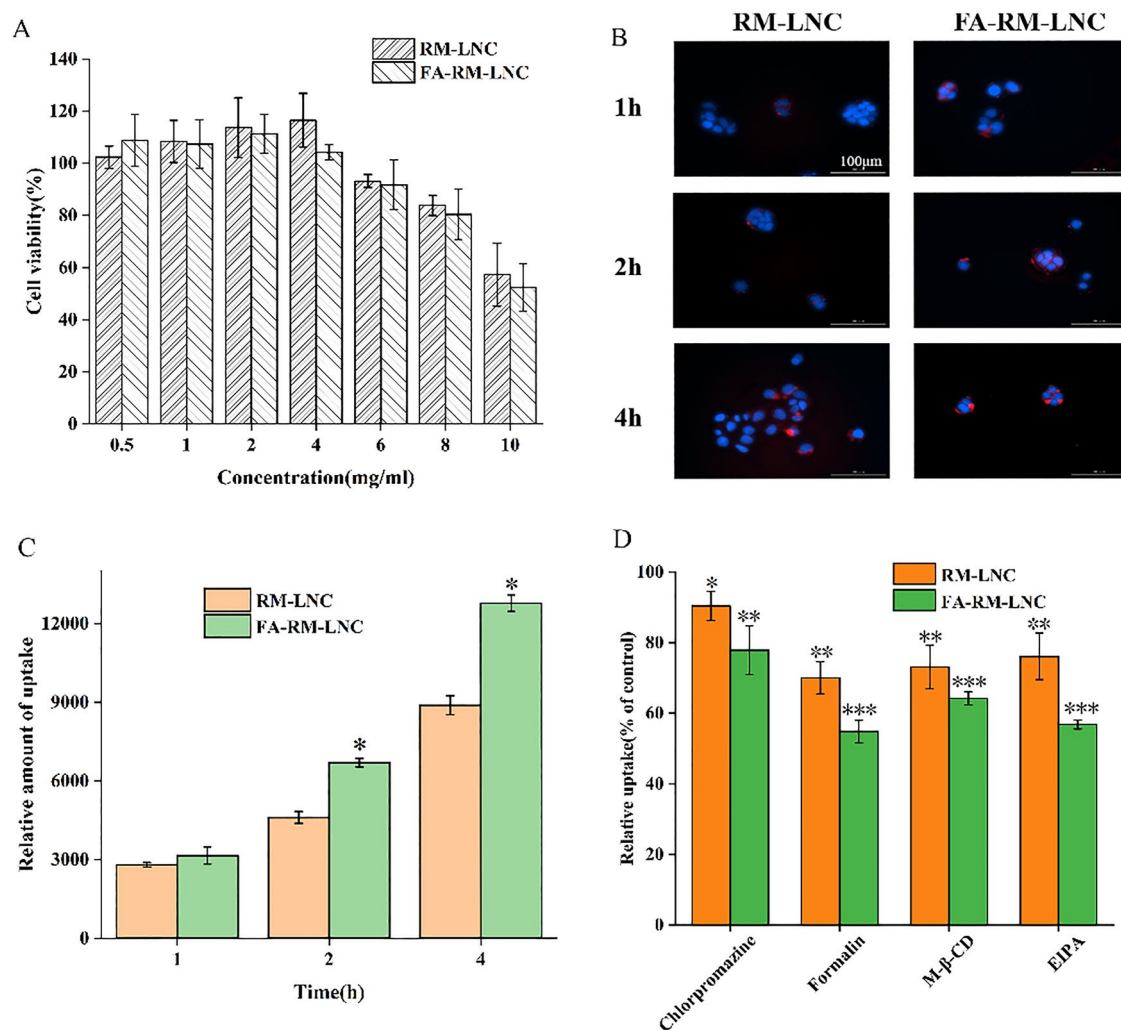


Figure 3. (A) Cell viability of Caco-2 cells after 24 h incubation with RM-LNC and FA-RM-LNC ($n=3$). (B) Cellular uptake study. Images of RM-LNC and FA-RM-LNC after co-incubation with Caco-2 cells. Scale bar: 100 μm . (C) Relative fluorescence intensity of DID in Caco-2 cells. Data are presented as mean \pm standard deviation ($n=3$). * $p < .05$, RM-LNC versus FA-RM-LNC. (D) Relative uptake of LNCs in the presence of different endocytosis inhibitors. Using the control group as the benchmark of 100%. * $p < .05$; ** $p < .01$; *** $p < .001$.

Table 2. P_{app} values when incubating different formulations with cell monolayers ($n=3$).

Formulations	$P_{\text{app}}(\text{cm/s}) \times 10^{-8}$
RM-LNC	6.81 ± 0.4
FA-RM-LNC	8.36 ± 0.41
DSPE-PEG-FA+RM-LNC	6.38 ± 0.53
DSPE-PEG-FA+FA-RM-LNC	5.6 ± 0.31

According to the literature, LNCs can be stored at low temperatures for up to six months (Aparicio-Blanco et al., 2019). Furthermore, the LNCs could maintain a stable particle size in simulated gastrointestinal fluids, which could be due to the fact that LNCs have a strong rigid shell that allows them to maintain their particle morphology in harsh environments. Even when the particles were subjected to PBS at 37 $^{\circ}\text{C}$, their size and PDI did not change significantly, which indicates good stability (Figure 2(A)). Furthermore, CD analyses showed that exenatide in nanoparticles prepared by different formulations could maintain its original conformation (Figure 2(B)), ensuring that the drug could exert its therapeutic effects *in vivo*. Based on the release profile

(Figure 2(C)), the LNCs prepared from polymeric materials exerted a slow-release effect on exenatide. Moreover, the modification of DSPE-PEG2000-FA did not significantly affect the release behavior of the drug compared to the unmodified formulation, which could be attributed to the fact that this modification material is not present in large quantities on the surface of the particles and does not affect the protective and retarding effect of the other polymeric materials on the drug. However, the stability of exenatide is affected to some extent during the release process, wherein the final cumulative release does not reach 100%. A similar release behavior was observed for LNCs (Xu et al., 2020a,b). *In vitro* release experiments also indirectly demonstrated that the reverse micelles containing exenatide were encapsulated into LNCs, with the particle structure as shown in Figure 1(A).

Cytotoxicity experiments showed that both RM-LNCs and FA-RM-LNCs were not significantly cytotoxic (Figure 3(A)). In Caco-2 cell uptake experiments, both modified and unmodified LNC showed a time-dependent uptake by cells, suggesting its strong association with the active transport system (Figure 3(B)). The fluorescence intensity of the FA-RM-LNC

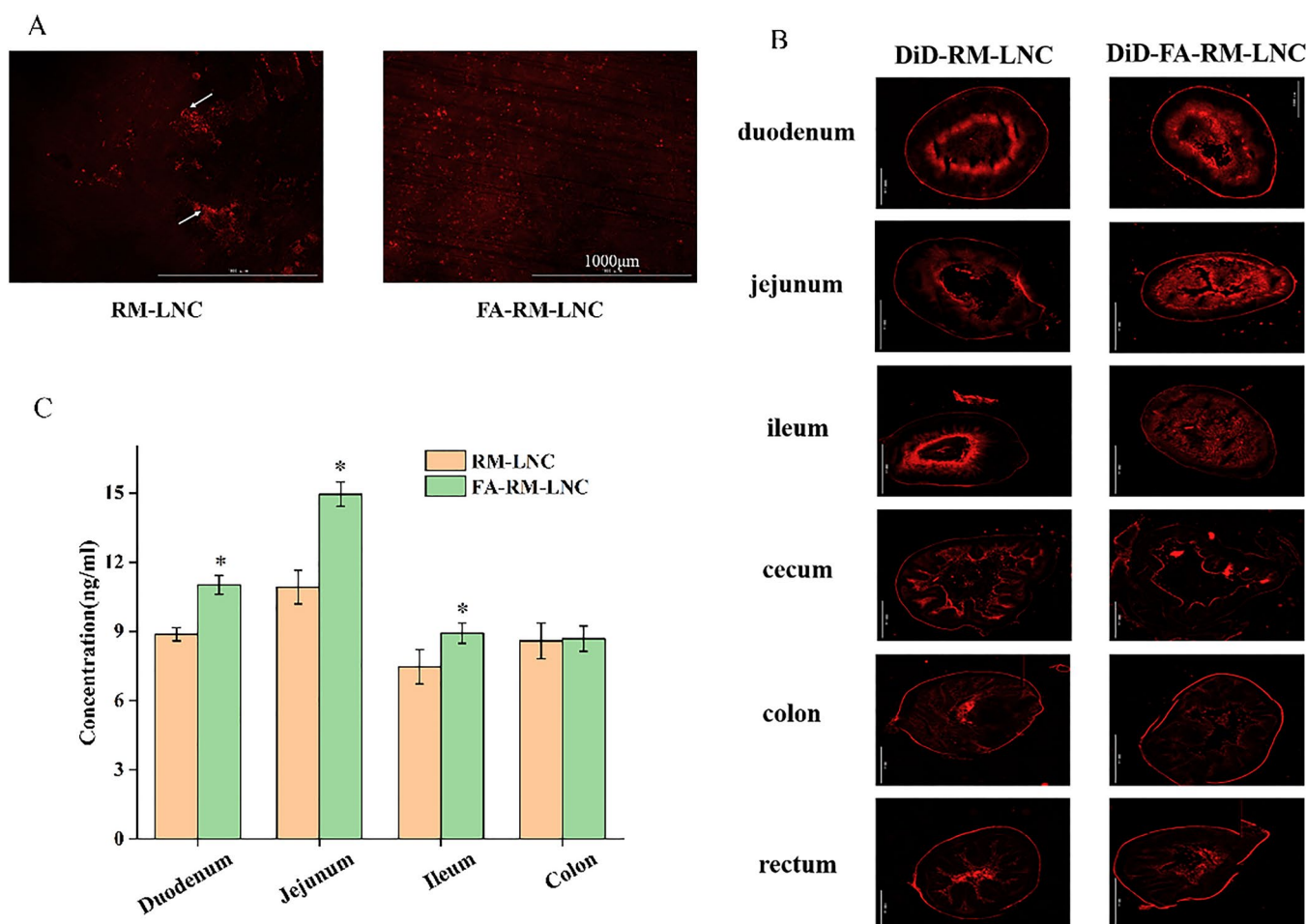


Figure 4. (A) Aggregation of nanoparticles in the mucus. (B) Complete image of the different segments of the intestine using the CYTATION imaging reader. (C) Absorption of LNCs in the flipped intestinal circulation *in vitro*. Compared with the RM-LNC group, $n=3$, $*p<.05$.

Table 3. Pharmacokinetic parameters of exenatide following the administration of different exenatide formulations (mean \pm standard deviation, $n=5$).

	Exenatide solution (oral)	RM-ELNC (oral)	FA-RM-LNC (oral)	Exenatide solution(s.c.)
Dose (ug/mL)	100	100	100	10
C_{max} (pg/mL)	101.51 \pm 11.69	132.19 \pm 9.1	188.25 \pm 10.36	378.75 \pm 5.25
T_{max} (h)	6	6	6	0.25
AUC (pgh/mL)	1534.48	2435.98	3121.93	4147.47
B_R (%)	3.7	5.87	7.53	100

group was higher than that of the RM-LNC group when observed at different time points, indicating that the DSPE-PEG-FA modification facilitated the cellular uptake of FA-RM-LNC. This phenomenon is likely to be driven by an increase in the amount of nanoparticles transported into Caco-2 cells, which was mediated by FA and induced more FA-RM-LNCs to be recognized by cells for uptake through specific recognition with small intestinal epithelial cells (Agrawal et al., 2014). Overall, the uptake of FA-RM-LNC was cellularly enhanced after modification with DSPE-PEG-FA compared to that of RM-LNCs (Figure 3(C)). Moreover, the uptake mechanism analysis suggests that active transport processes involved in adsorption and endocytosis could play an important role in the uptake of both preparations (Figure 3(D)). Notably, folic acid alters the uptake pathway of FA-RM-LNCs through specific ligand-receptor interactions, thus promoting the epithelial internalization of functionalized LNCs. The

results of trans-cellular transport (Table 2) suggest that the transport of RM-LNCs is independent of the presence of DSPE-PEG-FA and that the increase in FA-RM-LNC transport is mediated by the specific affinity of DSPE-PEG-FA for Caco-2 cells (Granja et al., 2019). Free DSPE-PEG-FA inhibits FA-RM-LNC transport by over-competing for Caco-2 cell surface receptors (Ashokkumar et al., 2007).

The relatively low aggregation of FA-RM-LNC in the mucus could be due to the fact that the particles themselves tend to be more electrically neutral in potential compared to those of RM-LNCs (Figure 4(A)). Nanocarriers smaller than 200 nm and with a PEG surface can exhibit high mucus permeability (Haddadzadegan et al., 2022). These favorable conditions could have weakened the aggregation of FA-RM-LNC in the mucus layer, which could also be attributed to the involvement of PEG in the composition of the surface rigid shell of LNCs (Figure 1(A)) and the involvement of PEG2000 in the modification of

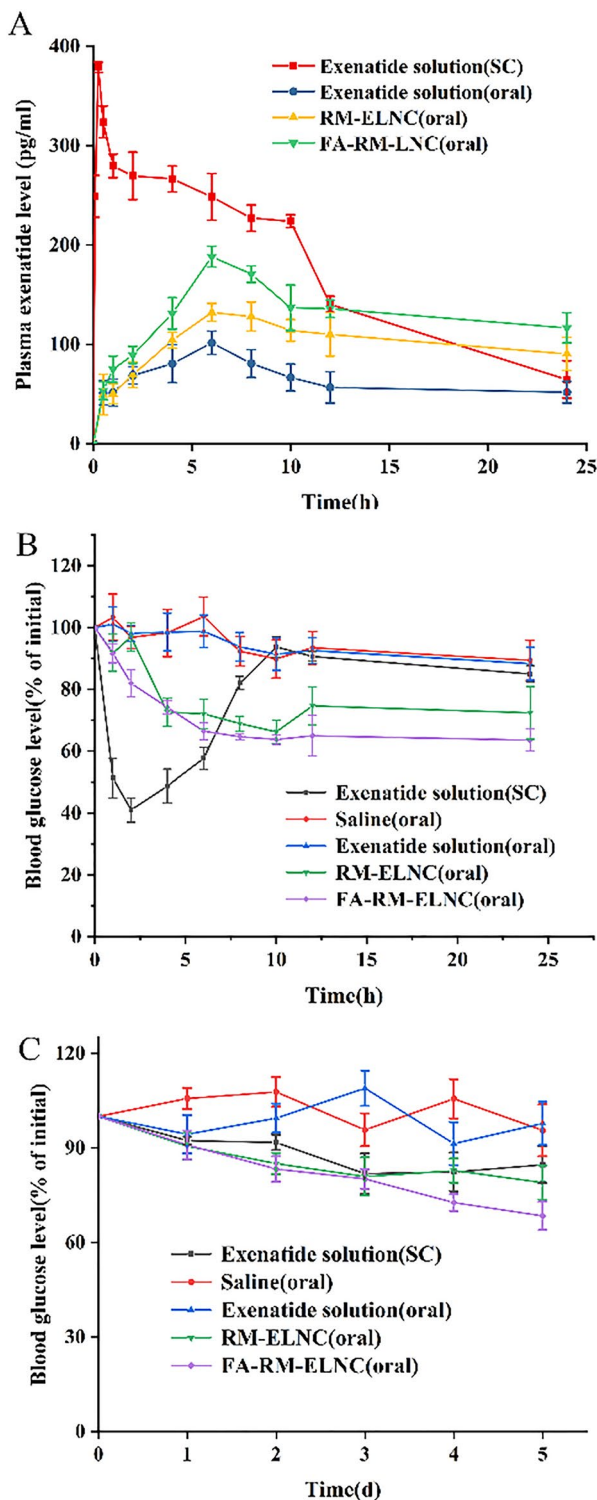


Figure 5. (A) Plasma levels of exenatide at different time points. The subcutaneous injection of exenatide solution was used as a positive control (mean \pm standard deviation, $n=5$). (B) Blood glucose levels in diabetic rats after a single administration. Subcutaneous injection of exenatide solution was used as a positive control (mean \pm standard deviation, $n=5$). (C) Blood glucose levels in diabetic rats after multiple dosing. The subcutaneous injection of exenatide solution was used as a positive control (mean \pm standard deviation, $n=5$).

the particle surface. The specific target binding of folic acid and enterocytes also resulted in higher absorption of FA-RM-LNC in the small intestine, especially at the duodenal and jejunal sites (Figure 4(C)). The better absorbability of the RM-LNC group at the large intestinal location could be explained by the fact that

only a small proportion of functionalized LNCs reached the large intestinal location *via* peristalsis compared to the amount of unmodified LNCs entering the large intestine (Figure 4(B)). Consistent with previous studies, the current results also suggest that FA is specifically recognized in the intestine by interacting with receptors on the surface of enterocytes, thus mediating the specific binding of FA-RM-LNCs to enterocytes and facilitating the absorption of nanoparticles in the small intestine.

These findings suggest that FA promotes interaction with small intestinal epithelial cells and boosts increased drug delivery into the small intestine. Moreover, the DSPE-PEG-FA modified nanocapsules greatly increased the bioavailability of exenatide *via* the oral route of administration (Table 3 and Figure 5(A)). Based on these results, it can be concluded that encapsulation with FA-RM-LNC is an effective method to protect exenatide and improve its intestinal epithelial permeation. We observed a significant hypoglycemic effect after the oral administration of FA-RM-ELNC compared to that of oral exenatide solution (Figure 5(B)). The hypoglycemic effect could be maintained for a longer period due to the modification of the particle surface with PEG2000 (Figure 5(C)). These results suggest that the encapsulation of FA-RM-LNC enhances the pharmacological effects of exenatide. The long-term hypoglycemic effect of orally administered FA-RM-ELNC could be partly attributed to the slow release of exenatide from the LNCs. The lack of significant changes in blood glucose levels following subcutaneous administration in multiple dosing trials could be related to the rapid absorption and rapid hypoglycemic effect following subcutaneous administration. This resulted in a rebound of the already lowered blood glucose levels at 12h of administration. Overall, the control of blood glucose was more stable with oral FA-RM-ELNC. Xu et al. report that LNCs triggered GLP-1 secretion in human and mouse cells as well as in mice (Xu et al., 2020a,b). The ability of RM-LNCs and FA-RM-LNCs to trigger endogenous GLP-1 secretion can be analyzed in future studies using more innovative colon-targeting preparations to enhance the level of endogenous GLP-1 secretion. Thus, combining this innovative delivery system to increase endogenous GLP-1 secretion and increase the oral bioavailability of the GLP-1 analog exenatide provides new perspectives for the treatment of diabetes.

5. Conclusion

In this study, LNCs were stable *in vitro* and had a good affinity to epithelial cells, thus enhancing intracellularization and transcellular transport. *In vivo* experiments also showed that the oral administration of FA-RM-ELNC exhibited a good hypoglycemic effect in type 2 diabetic mice. Furthermore, the prepared FA-RM-LNC has promising therapeutic potential for the oral delivery of exenatide. Nonetheless, further investigation should be undertaken into the biosafety of this delivery system, its ability to be used to deliver other proteins peptides and strategies to stimulate endogenous GLP-1

secretion. This study provides promising prospects for developing treatments for diabetes.

Ethical approval

All animal experiments were approved by the Experimental Animal Ethics Committee of the College of Pharmacy, Yantai University.

Acknowledgments

We thank Bullet Edits Company for editing the English text of a draft of this manuscript.

Disclosure statement

The authors declare no competing financial interest.

Funding

This work was financially supported by the Yantai University Doctoral Program (SM20B35) and the Natural Science Foundation of Shandong Province (ZR2021MH395).

ORCID

Yanan Shi  <http://orcid.org/0000-0002-4427-6493>

References

- Agrawal AK, Harde H, Thanki K, Jain S. (2014). Improved stability and antidiabetic potential of insulin containing folic acid functionalized polymer stabilized multilayered liposomes following oral administration. *Biomacromolecules* 15:1–12.
- Aparicio-Blanco J, Sebastian V, Rodriguez-Amaro M, et al. (2019). Size-tailored design of highly monodisperse lipid nanocapsules for drug delivery. *J Biomed Nanotechnol* 15:1149–61.
- Ashokkumar B, Mohammed ZM, Vaziri ND, Said HM. (2007). Effect of folate oversupplementation on folate uptake by human intestinal and renal epithelial cells. *Am J Clin Nutr* 86:159–66.
- Drucker DJ. (2020). Advances in oral peptide therapeutics. *Nat Rev Drug Discov* 19:277–89.
- Fosgerau K, Hoffmann T. (2015). Peptide therapeutics: current status and future directions. *Drug Discov Today* 20:122–8.
- Granja A, Neves AR, Sousa CT, et al. (2019). EGCG intestinal absorption and oral bioavailability enhancement using folic acid-functionalized nanostructured lipid carriers. *Heliyon* 5:e02020.
- Groo AC, Saulnier P, Gimel JC, et al. (2013). Fate of paclitaxel lipid nanocapsules in intestinal mucus in view of their oral delivery. *Int J Nanomedicine* 8:4291–302.
- Guo S, Liang Y, Liu L, et al. (2021). Research on the fate of polymeric nanoparticles in the process of the intestinal absorption based on model nanoparticles with various characteristics: size, surface charge and pro-hydrophobics. *J Nanobiotechnology* 19:32.
- Haddadzadegan S, Dorkoosh F, Bernkop-Schnürch A. (2022). Oral delivery of therapeutic peptides and proteins: technology landscape of lipid-based nanocarriers. *Adv Drug Deliv Rev* 182:114097.
- Huynh NT, Passirani C, Saulnier P, Benoit JP. (2009). Lipid nanocapsules: a new platform for nanomedicine. *Int J Pharm* 379:201–9.
- Jain D, Mahammad SS, Singh PP, Kodipyaka R. (2019). A review on parenteral delivery of peptides and proteins. *Drug Dev Ind Pharm* 45:1403–20.
- Jain KK. (2020). An overview of drug delivery systems. *Methods Mol Biol* 2059:1–54.
- Jain S, Rath V, Jain AK, et al. (2012). Folate-decorated PLGA nanoparticles as a rationally designed vehicle for the oral delivery of insulin. *Nanomedicine (Lond)* 7:1311–37.
- Labrak Y, Heurtault B, Frisch B, et al. (2022). Impact of anti-PDGFR α antibody surface functionalization on LNC uptake by oligodendrocyte progenitor cells. *Int J Pharm* 618:121623.
- Laine AL, Gravier J, Henry M, et al. (2014). Conventional versus stealth lipid nanoparticles: formulation and in vivo fate prediction through FRET monitoring. *J Control Release* 188:1–8.
- Lau JL, Dunn MK. (2018). Therapeutic peptides: historical perspectives, current development trends, and future directions. *Bioorg Med Chem* 26:2700–7.
- Li J, Zhang Y, Yu M, et al. (2022). The upregulated intestinal folate transporters direct the uptake of ligand-modified nanoparticles for enhanced oral insulin delivery. *Acta Pharm Sin B* 12:1460–72.
- Liang Y, Ding R, Wang H, et al. (2022). Orally administered intelligent self-ablating nanoparticles: a new approach to improve drug cellular uptake and intestinal absorption. *Drug Deliv* 29:305–15.
- Mittal G, Carswell H, Brett R, et al. (2011). Development and evaluation of polymer nanoparticles for oral delivery of estradiol to rat brain in a model of Alzheimer's pathology. *J Control Release* 150:220–8.
- Nasr M, Abdel-Hamid S. (2015). Lipid based nanocapsules: a multitude of biomedical applications. *Curr Pharm Biotechnol* 16:322–32.
- Nauck MA, Quast DR, Wefers J, Meier JJ. (2021). GLP-1 receptor agonists in the treatment of type 2 diabetes – state-of-the-art. *Molecular Metabolism* 46:101102.
- Perrier T, Saulnier P, Fouchet F, et al. (2010). Post-insertion into Lipid NanoCapsules (LNCs): from experimental aspects to mechanisms. *Int J Pharm* 396:204–9.
- Radwan SAA, El-Maaday WH, ElMeshad AN, et al. (2020). Impact of reverse micelle loaded lipid nanocapsules on the delivery of gallic acid into activated hepatic stellate cells: a promising therapeutic approach for hepatic fibrosis. *Pharm Res* 37:180.
- Roger E, Gimel JC, Bensley C, et al. (2017). Lipid nanocapsules maintain full integrity after crossing a human intestinal epithelium model. *J Control Release* 253:11–8.
- Roger E, Lagarce F, Garcion E, Benoit JP. (2009). Lipid nanocarriers improve paclitaxel transport throughout human intestinal epithelial cells by using vesicle-mediated transcytosis. *J Control Release* 140:174–81.
- Sheng J, He H, Han L, et al. (2016). Enhancing insulin oral absorption by using mucoadhesive nanoparticles loaded with LMWP-linked insulin conjugates. *J Control Release* 233:181–90.
- Song Y, Shi Y, Zhang L, et al. (2019). Synthesis of CSK-DEX-PLGA nanoparticles for the oral delivery of exenatide to improve its mucus penetration and intestinal absorption. *Mol Pharm* 16:518–32.
- Topin-Ruiz S, Mellinger A, Lepeltier E, et al. (2021). p722 ferrocifen loaded lipid nanocapsules improve survival of murine xenografted-melanoma via a potentiation of apoptosis and an activation of CD8(+) T lymphocytes. *Int J Pharm* 593:120111.
- Tsakiris N, Papavasileiou M, Bozzato E, et al. (2019). Combinational drug-loaded lipid nanocapsules for the treatment of cancer. *Int J Pharm* 569:118588.
- Valdes-Ramos R, Guadarrama-Lopez AL, Martinez-Carrillo BE, Benitez-Arciniega AD. (2015). Vitamins and type 2 diabetes mellitus. *Endocr Metab Immune Disord Drug Targets* 15:54–63.
- Xu Y, De Keersmaecker H, Braeckmans K, et al. (2020a). Targeted nanoparticles towards increased L cell stimulation as a strategy to improve oral peptide delivery in incretin-based diabetes treatment. *Biomaterials* 255:120209.
- Xu Y, Van Hul M, Suriano F, et al. (2020b). Novel strategy for oral peptide delivery in incretin-based diabetes treatment. *Gut* 69:911–9.
- Zaman R, Islam RA, Ibnat N, et al. (2019). Current strategies in extending half-lives of therapeutic proteins. *J Control Release* 301:176–89.
- Zhu X, Wu J, Shan W, et al. (2016). Polymeric nanoparticles amenable to simultaneous installation of exterior targeting and interior therapeutic proteins. *Angew Chem Int Ed Engl* 55:3309–12.